

# Kinetics of Capillary Extraction of Organic Vehicle from Ceramic Bodies. Part II: Partitioning between Porous Media

Y. Bao & J. R. G. Evans

Department of Materials Technology, Brunel University, Uxbridge, Middlesex UB8 3PH, UK

(Received 14 January 1991; accepted 18 March 1991)

## Abstract

*An attempt was made to quantify the one-dimensional flow of molten wax from a ceramic body into a powder bed using permeability data deduced in Part I. The flow curve may be divided into three stages: (i) a transient stage of very rapid flow; (ii) a stable stage during which the majority of the wax is extracted, which is parabolic with time and is characterized by a sorption constant as for wax extraction from an unlimited supply; (iii) a reduced velocity stage in which the residual wax in the body approaches the pendular configuration (in which isolated liquid lenses exist at particle junctions). It was found that the residual wax in the body remained uniformly distributed during extraction and its saturation decayed. On the other hand, wax flow into the powder bed approximated to a one-dimensional column of fixed saturation. The absence of a permeability–saturation relationship for diverse powders is one of the main obstructions to a general theory of capillary extraction of binder, and this limited the agreement between measured and calculated sorption constants.*

*Es wurde versucht, das Fließverhalten geschmolzenen Wachses von einem keramischen Formkörper in ein Pulverbett mit den in Teil I erhaltenen Permeabilitätsdaten anhand eindimensionaler Geometrie zu quantifizieren. Die Fließkurve kann in drei Bereiche unterteilt werden: (a) einen Übergangsbereich mit sehr schnellem Fließen; (b) einen stationären Bereich mit parabolischem Zeitgesetz während dem der Hauptanteil des Wachses entfernt wird, der durch eine Sorptionskonstante beschrieben werden kann und bei dem beständig Wachs nachgeliefert wird; (c) einen Bereich mit einer kleineren Geschwindigkeit in dem das restliche Wachs im Formkörper sich homogen verteilt. In diesem Stadium bilden sich an den*

*Kontaktstellen der Teilchen voneinander isolierte Hälse der flüssigen Phase aus. Es hat sich gezeigt, daß dieses restliche Wachs im Formkörper während des Entfernens homogen verteilt bleibt, aber die Gesamtmenge abnimmt. Andererseits entspricht das Fließverhalten des Wachses in die Pulverschüttung nahezu dem Modell einer eindimensionalen Säule mit einer bestimmten Sättigung. Die Abwesenheit einer Permeabilitäts–Sättigungs Beziehung für die verschiedenen Pulver stellt eines der Haupthindernisse zu einer allgemeinen Theorie der Binderentfernung durch Kapillarkräfte dar und dies ist der Grund für die begrenzte Übereinstimmung zwischen gemessenen und berechneten Sorptionskonstanten.*

*On a conduit des travaux visant à quantifier l'écoulement unidimensionnel de la cire fondue d'une pièce céramique dans un lit de poudre en utilisant les valeurs de perméabilité de la partie I. La courbe d'écoulement peut être décomposée en trois étapes: (i) étape transitoire d'écoulement très rapide; (ii) étape stable durant laquelle la plus grande partie de la cire est extraite, qui est parabolique en fonction du temps et est caractérisée par une constante de sorption comparable au cas de l'extraction de cire en alimentation continue; (iii) étape à vitesse réduite pendant laquelle la cire résiduelle dans la pièce approche la configuration pendulaire (dans laquelle des ménisques de liquide isolés se trouvent aux jonctions entre particules). On a trouvé que la cire résiduelle restait distribuée de façon uniforme lors de l'extraction et que sa saturation s'affaiblissait. D'autre part, l'écoulement de cire au sein du lit de poudre s'approche d'une colonne unidimensionnelle de saturation fixe. L'absence de relation entre la perméabilité et la saturation pour différentes poudres est l'un des obstacles majeurs à l'édification d'une théorie générale de l'extraction capillaire du liant, ce*

qui restreint l'accord entre les valeurs de constante de sorption mesurée et calculée.

## 1 Introduction

The objective of this work is to develop the quantitative basis for extraction of organic vehicle from moulded ceramic bodies, first by examination of the factors affecting flow in powder beds<sup>1</sup> and then by application of these principles to the industrially relevant situation wherein a ceramic body is brought into contact with a porous bed or tile and the organic vehicle partitions itself between the two media.

Previous work on the extraction of organic vehicle from ceramic bodies by capillary flow into powder beds has shown that only a fraction of the available pore space in the powder bed is used and that, even in a one-dimensional flow experiment, columnar flow in the ceramic body does not appear to occur. Saturation of the ceramic cylinder after partial depletion of the vehicle was constant in the radial and longitudinal directions.<sup>2</sup>

The analysis of wax flow in powder beds from an unlimited supply has highlighted the difficulty of applying general expressions for permeability and average capillary pressure to diverse powders, and hence the serious problem of arriving at a useful quantitative model for the extraction process. It was necessary to resort to experiment to acquire the permeability values needed to quantify the flow. In the present work this data is applied to the extraction of vehicle from ceramic bodies.

## 2 Flow in the Coupled System

Using subscripts p for powder bed and d for the ceramic disc, and considering a length  $H$  of liquid column inside the ceramic body and length  $x$  of liquid column inside the powder at time  $t$ , Darcy's law can be applied to flow in the body and powder bed as follows:

$$\left(\frac{dV}{dt}\right)_d = -\frac{K_d A (P_{cd} - P_{co})}{\eta \sqrt{2} H} \quad (1a)$$

$$\left(\frac{dV}{dt}\right)_p = -\frac{K_p A (P_{co} - P_{cp})}{\eta \sqrt{2} x} \quad (1b)$$

where  $P_{co}$  is the average capillary pressure at the interface and  $dV/dt$  is the volumetric flow rate. For

continuity of flow

$$\left(\frac{dV}{dt}\right)_d = \left(\frac{dV}{dt}\right)_p = \frac{dV}{dt} \quad (2)$$

Rearranging eqns (1a) and (1b) and adding

$$\frac{dV}{dt} = \frac{K_d K_p}{K_p H + K_d x} \frac{A \Delta P_c}{\sqrt{2} \eta} \quad (3)$$

where  $\Delta P_c$  is the positive average capillary pressure difference, eqn (3) can be expressed as

$$\frac{dV}{dt} = K_{\text{eff}} \frac{A \Delta P_c}{\sqrt{2} \eta L} \quad (4)$$

where  $K_{\text{eff}}$  is an effective permeability for the coupled system and  $L$  is the total length of the liquid column. Thus

$$\frac{1}{K_{\text{eff}}} = \frac{H}{L} \frac{1}{K_d} + \frac{x}{L} \frac{1}{K_p} \quad (5)$$

since  $L = x + H$ . Alternatively, putting  $f = x/L$ ,

$$\frac{1}{K_{\text{eff}}} = \frac{1-f}{K_d} + \frac{f}{K_p} \quad (6)$$

Clearly  $f$  and hence  $K_{\text{eff}}$  can vary with time for two reasons: (i)  $K_d \neq K_p$  and (ii)  $K_d = K_p$  but  $E_d s_d \neq E_p s_p$ , where  $E$  is the total porosity of the powder assembly and  $s$  is the saturation.

For the three limiting situations previously discussed,<sup>2</sup>  $K_{\text{eff}}$  can be related directly to  $K_d$  or  $K_p$  without time dependence:

$$\text{for } K_p = K_d \quad K_{\text{eff}} = K_p = K_d \quad (7a)$$

$$\text{for } K_p \gg K_d \quad \frac{K_{\text{eff}}}{L} = \frac{K_d}{H} \quad (7b)$$

$$\text{for } K_p \ll K_d \quad \frac{K_{\text{eff}}}{L} = \frac{K_p}{x} \quad (7c)$$

For the third case eqn (4) can be integrated to show the time dependence of the volume of wax transferred per unit cross-sectional area of the flow path:

$$v = V/A = Kt^{1/2} \quad (8)$$

where  $K$  is a sorption constant analogous to that used for sorption from an unlimited supply.<sup>1</sup> The sorption constant is given by

$$K = \left( \frac{\sqrt{2} K_p \Delta P_c E_p s_p}{\eta} \right)^{1/2} \quad (9)$$

and, provided it can be shown that  $K_p \ll K_d$ , it differs only in that the driving force for flow now incorporates the opposing capillary pressure of the ceramic body. The actual value of  $K_p$  may also be lower than for sorption from an unlimited supply because saturation of the powder may be lower.

### 3 Experimental Details

#### 3.1 Materials

The alumina powders were the same as those tested in Part I.<sup>1</sup> The paraffin wax was also from the same batch as that used previously. The wax viscosity at various temperatures was measured using a 'U' tube viscometer following the standard procedure.<sup>3</sup>

#### 3.2 Preparation of ceramic bodies

The ceramic powder (MA2LS) and paraffin wax were compounded by twin-screw extrusion using the procedure previously described,<sup>4</sup> with barrel temperatures of 80, 80, 110 and 110°C, feed to exit and a screw speed of 60 rpm. The extrudate was water cooled and dried in a vacuum oven. The exact composition was calculated from ashing results. Discs of 25 mm diameter and 16 mm thickness were prepared by compression moulding at 60°C and under 10–14 MPa pressure.

#### 3.3 Wax extraction

The plunger used for wax extraction, which allows the measurement of one-dimensional flow, has been described previously (Fig. 1 of Ref. 1). The barrel was packed with powder to a predetermined relative density and both ceramic body and powder bed were preheated. The extraction time was measured from the moment when the ceramic body contacted the powder bed. There was sufficient leakage past the plunger to prevent back pressure developing. The experiments were done in a Townsen & Mercer oven with a glass window. The temperature of the barrel was recorded using a type K thermocouple. The amount of binder removed was determined from the weight loss of the ceramic body and the distribution of wax in the powder bed was obtained from the ashing of sections of the bed. These experiments were carried out under conditions of constant temperature and varying time. Several temperatures and several powder beds were also investigated. The accuracy associated with the measurements of temperature and weight were  $\pm 1^\circ\text{C}$  and  $\pm 1\text{ mg}$ , respectively.

The ceramic body was also cut into sections and ashed to determine the wax distribution after extraction in the direction of flow.

### 4 Results and Discussion

#### 4.1 Measurement of sorption constant

Ashing experiments showed that the ceramic body contained 16.5 wt% wax, corresponding to 46.2

**Table 1.** Amount of wax removed after 6 h at 80°C expressed as a percentage of that initially present

Powder bed	Ceramic body (%)	
	RA6	MA2LS
RA6	14.5	69.5
LA75	10.7	20.3
MA2LS	(not tested)	11.6
LA150	(not tested)	20.1

vol%. Each disc therefore contains 3.32 g wax. The cross-sectional area of the flow path was  $5.07 \times 10^{-4} \text{ m}^2$ .

Of the coarse and fine powder categories investigated in Part I,<sup>1</sup> MA2LS and LA150 presented very low sorption constants from an unlimited wax supply and were therefore not used for quantitative study in the present work. This selection is confirmed by results in Table 1 for the amount of wax extracted after 6 h at 80°C. For the same reason RA6 was not selected for the ceramic body. The measurement of very small transfers of wax introduces errors which make the comparison with theory ambiguous.

Flow curves were obtained at 80°C using the ceramic body prepared from MA2LS with RA6 and LA75 powder beds, and these are shown in Fig. 1 using the same format as that used to describe flow from an unlimited supply (see Fig. 7 of Part I). It is therefore instructive to see if they obey the same parabolic law. Figure 2 shows  $v(x)$  as a function of the square root of time and should be compared with Fig. 4 of Part I. It is clear that during the removal of wax from a ceramic body there are three stages.

- (i) An initial transient stage occurs at the beginning of binder removal which does not obey the same parabolic relationship that characterizes the bulk of the extraction. When the ceramic body first touches the powder bed it is not only saturated with wax but there is an excess of wax over and above that needed to fill the interstitial space between contacting particles. This excess must be removed before the particles make contact and the full opposing capillary pressure of the body is established. This, however, accounts for only a small fraction of wax and a further explanation of the transient stage emerges from consideration of the form of the Leverett function curve and will be discussed. The initial flow is comparable to the rate obtained from an unlimited supply. In Fig. 2 the intercept with the ordinate is the result of this initial transient stage.

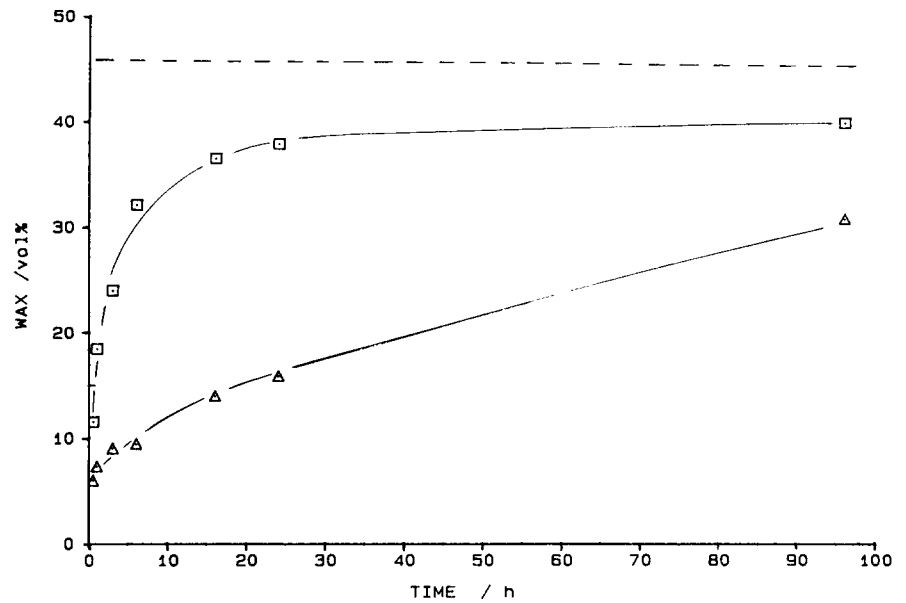


**Fig. 1.** Kinetics of wax extraction from MA2LS ceramic bodies at 80°C. Powder beds: □, RA6; △, LA75. (Wax removed expressed as a percentage of the volume of the ceramic body. Initial vol.% wax = 46.2.)

- (ii) Stage 2 is termed the stable stage, during which the majority of wax is removed from the body and generally lasts for a long time. This stage gives rise to a parabolic flow curve with an associated sorption constant which is considerably lower than that obtained for flow from an unlimited supply. This stage, being the most important, will be discussed in more detail.
- (iii) Finally, when the majority of the binder has been removed (generally more than 66%) the parabolic curve flattens out, giving a reduced velocity stage in which the residual wax in the ceramic body is considered to reach the pendular configuration. At this stage the number of connecting channels which allow the wax to migrate both within the body and

across the interface diminishes rapidly and discrete liquid bridges remain between particles. Only the smallest pores remain filled. Furthermore, from the form of the Leverett function the opposing capillary pressure of the body increases steeply in this stage.

The modified flow equation can therefore be expressed in the form

$$v = v_0 + K(t - t_0)^{1/2} \tag{10}$$

if the final reduced velocity stage is not included, where  $v_0$  represents the amount of wax extracted in the transient stage and  $t_0$  is the time for which the transient stage lasts. Since  $t_0$  is very small the majority of flow can be characterized by

$$v = v_0 + Kt^{1/2} \tag{11}$$

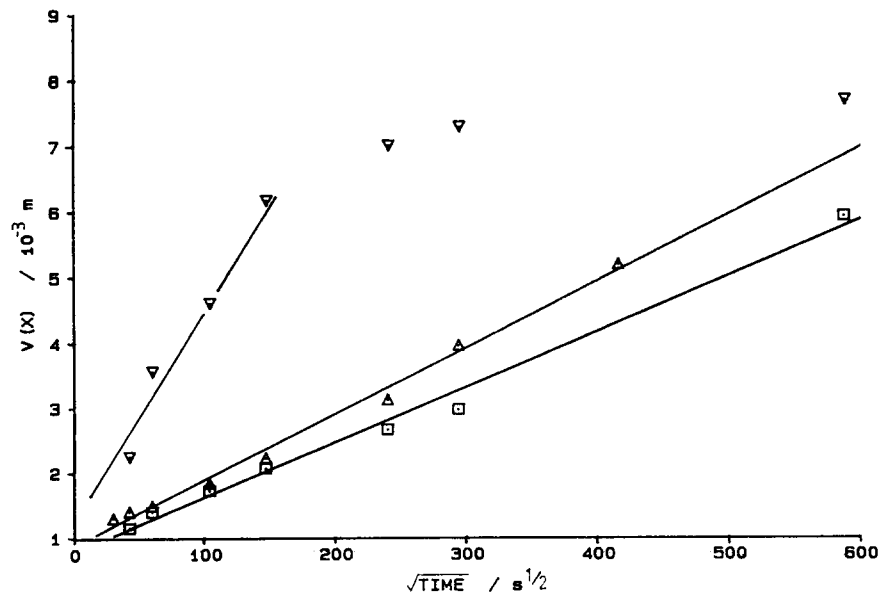


**Fig. 2.** Volume of wax extracted from MA2LS body per unit area of cross-section, expressed as a function of square root of time for ▽, RA6 powder bed at 80°C; □, LA75 powder bed at 80°C and △, at 100°C.

**Table 2.** Comparison of sorption constants and average saturation for the unlimited supply condition and for binder extraction

	Powder bed	
	RA6	LA75
Unlimited supply		
Sorption constant ( $\text{m s}^{-1/2}$ )	$6.96 \times 10^{-4}$	$1.11 \times 10^{-3}$
Period of measurement (min)	10	10
Available porosity (%)	70	71
Average saturation	1.00	0.88
Extraction from MA2LS body		
Sorption constant ( $\text{m s}^{-1/2}$ )	$3.39 \times 10^{-5}$	$8.62 \times 10^{-6}$
Stable stage duration (h)	~10	~100
Available porosity (%)	70	71
Average saturation	0.54	0.41

from which the sorption constant  $K$  can be obtained by linear regression during the stable stage. Table 2 compares the sorption constant deduced from an unlimited supply with that obtained from the extraction process. The sorption constant for both powders is considerably reduced when the powder bed is used to draw wax from the ceramic body, and the work which follows attempts to account for the new sorption constant.

#### 4.2 Effective porosity and saturation of the powder bed

After fixed periods of extraction the experiments were terminated and sections of the powder bed were removed from the cylinder using the screwed plunger. These were ashed to  $600^\circ\text{C}$  in air and the wax content was expressed as weight fraction based on the apparent weight of the powder bed. These results are shown in Fig. 3 as a function of distance from the interface.

Like the flow from an unlimited supply, the movement in the powder bed corresponds to columnar flow. Although the data for the RA6 powder bed appears to show a slight concentration gradient, the deviation from constant saturation is close to the experimental error associated with the ashing of small samples. The exact form of the concentration gradient at the end of the column cannot be clearly resolved because of the size of sections of powder bed taken and the problem of obtaining a clean slice. The average saturations are, however, much lower than for the unlimited supply condition and are summarized in Table 2. The results for these two powders are therefore quite striking; the sorption constant for the coarse LA75 is much lower than that for the fine RA6 for extraction, whereas for flow from an unlimited supply the reverse is the case.

Under conditions of extraction the reduction in saturation and in sorption constant can be explained from capillary theory. The ceramic body exerts an opposing capillary pressure not present in the case of sorption from an unlimited supply. The reduction in saturation of the powder bed results in a reduced permeability. In addition, there may be a surface mass-transfer resistance at the interface.

The presence of an opposing capillary pressure introduced by the ceramic body has a direct influence on average saturation of the powder bed. The average capillary pressures deduced in Part I<sup>1</sup> conceal a wide variation in microscopic capillary pressures which arise from different pore sizes. The latter are brought about *inter alia* by variations in particle size of the powder bed. Even for relatively narrow distributions, however, large differences in pore size can originate from non-uniform packing of the bed, such as that resulting from agglomeration or from particle bridging. Only those capillaries in the powder bed which are capable of exerting a capillary pressure greater than the opposing pressure from the body can therefore take part in extraction, and for this reason saturation of the powder bed is reduced.

#### 4.3 Saturation of the ceramic body

The distribution of residual wax in the ceramic body was also measured using experiments terminated at various times. Figure 4 shows that within the experimental errors the wax is uniformly distributed throughout the body at all times during extraction, and wax is lost, not by the flow of a column of liquid as previously thought<sup>5</sup> but by a uniform decrease in saturation. Previous work showed that the uniform longitudinal saturation was accompanied by a uniform radial saturation.<sup>2</sup> The implication of Fig. 4 is that the wax redistributes itself through the action of local pressure differences tending to fill the smaller pores, as discussed by Shaw.<sup>6</sup> This redistribution appears to offer less resistance to flow than occurs for transport into the powder bed.

Like the powder bed, the ceramic body is assumed to be another capillary assembly. The body exerts an opposing average capillary pressure and as wax emerges from the body its saturation decreases and the average capillary pressure changes with saturation in a manner described by the Leverett function for drainage<sup>7</sup> (reproduced in Ref. 1, Fig. 6). From Fig. 2  $v_0$  corresponds to approximately 9% of the wax in the ceramic body, indicating that saturation is approximately 91% at the start of the stable stage. The stable stage finishes when approximately 76% of wax has been removed, corresponding to a

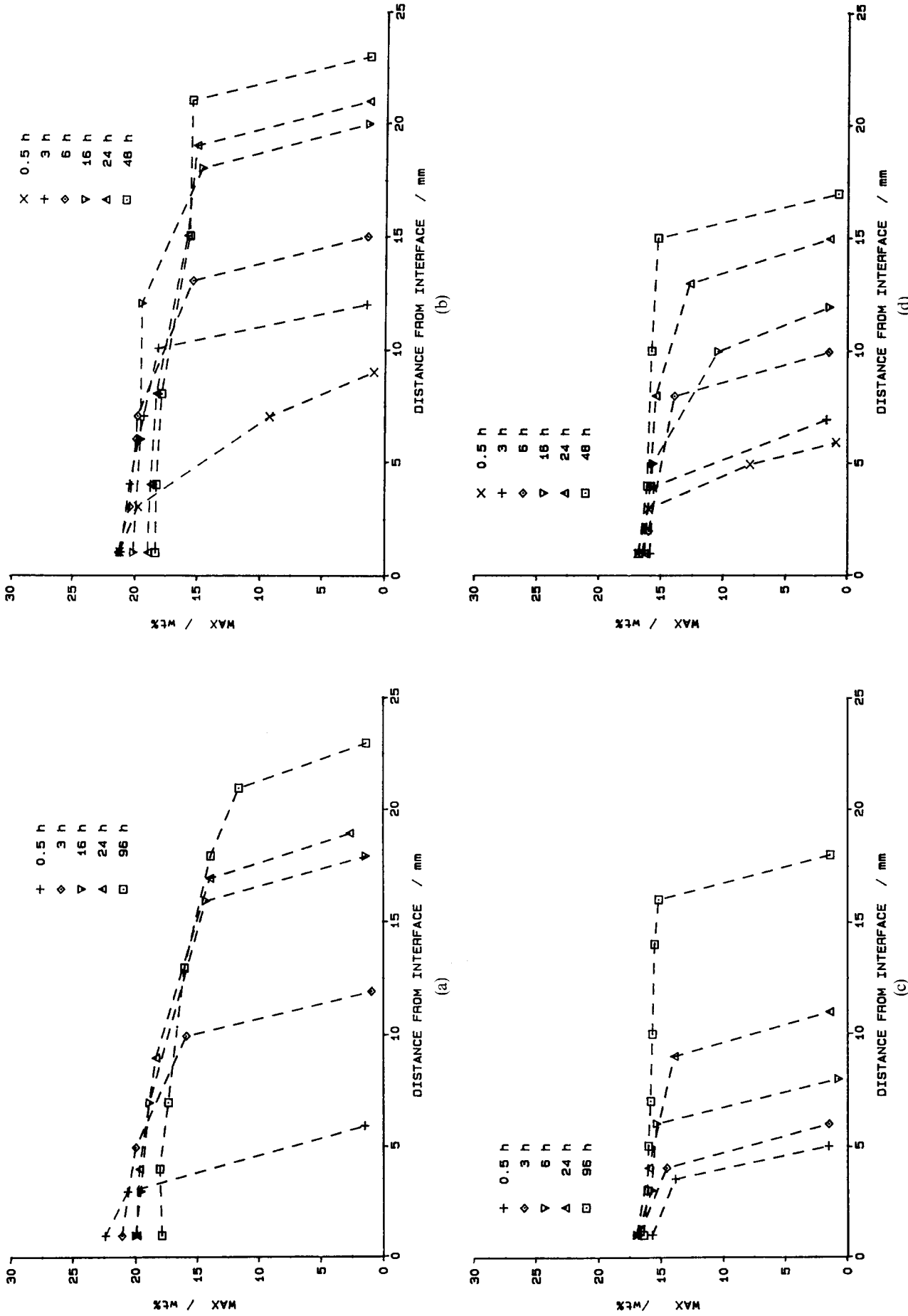
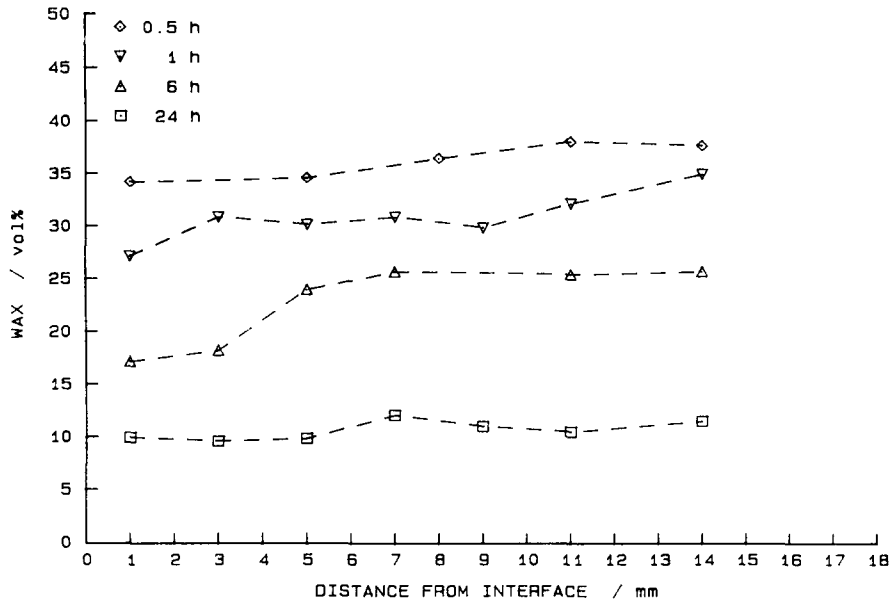
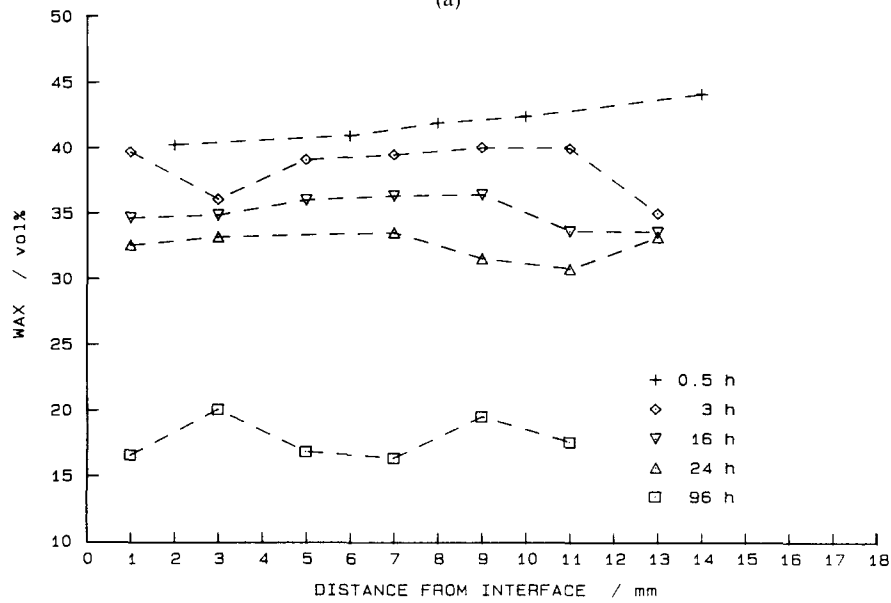


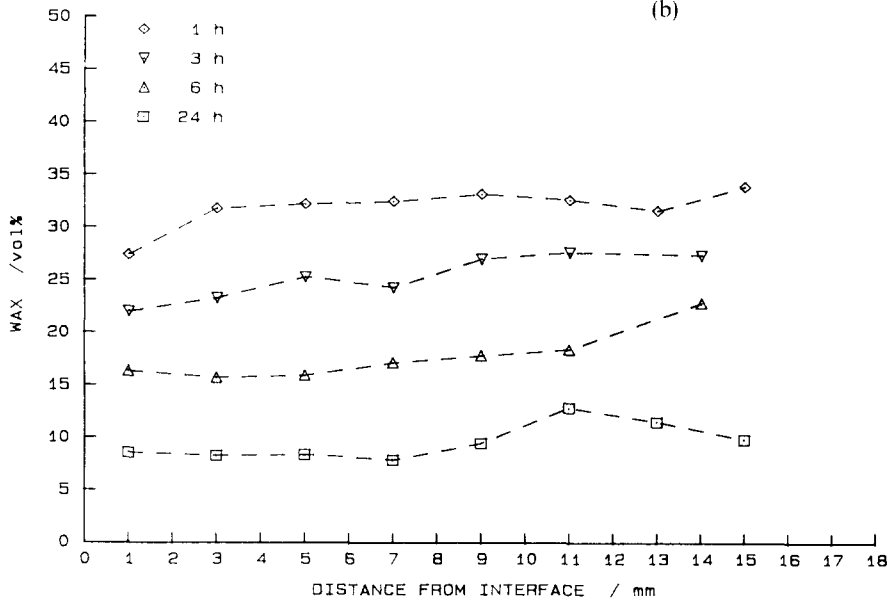
Fig. 3. Wax content of sections of powder bed at various times during the extraction process (wt% wax based on the weight of a section of the powder bed). For extraction from MA2LS body (a) into RA6 powder bed at 80°C and (b) at 100°C, (c) into LA75 powder bed at 80°C and (d) at 100°C.



(a)



(b)



(c)

**Fig. 4.** Distribution of residual wax in the ceramic body at various stages during the extraction process (vol.% wax based on the volume of the ceramic body). For extraction from MA2LS body (a) into RA6 powder bed at 80°C, (b) into LA75 powder bed at 80°C and (c) at 100°C.

saturation of 24%. The drainage curve from the Leverett function is almost flat in the interval 24–91% saturation, and this is the reason why the stable stage presents a parabolic flow curve. For the following conditions (i) constant saturation in the powder bed, (ii) powder bed permeability controlling flow, (iii) constant capillary pressure in the powder bed and (iv), from the Leverett function, constant opposing pressure, the parameters that comprise the sorption constant are invariant and so eqn (8) is obeyed.

#### 4.4 Comparison of calculated and measured sorption constant

The sorption constant in eqn (8) may be calculated for the case of powder bed control, provided  $K_p$  and  $\Delta P_c$  are known. The capillary pressure of powder assemblies can be found from the Leverett function<sup>7</sup> at various saturations in terms of the permeability and porosity at full saturation. The problem with  $K_p$  is that, unlike the situation for sorption from an unlimited supply, saturations of the powder beds are very low. Permeability of the powder bed as a function of porosity is known for a narrow range of porosity from Part I (eqns (26)–(28)), but there are two difficulties in using these equations in the present context. First, the pore size distribution of the filled pores at low saturation may not correspond exactly with the pore size distribution at full saturation in a powder which has been compressed to the same total porosity. Secondly, the use of eqns (26)–(28) (Part I) involves extrapolation to the low effective porosity levels encountered here. Permeability as a function of saturation has been obtained for various sands,<sup>8</sup> but the curve is claimed to be sensitive to particle size distribution. When permeabilities of these powder beds were calculated from it, very high values were obtained, corresponding to vanishingly small values for  $\Delta P_c$ . The permeability–saturation curve for a powder is likely to be sensitive to pore size distribution, and hence to particle size

distribution. The absence of a general relationship reveals itself as a major obstruction to a general theory of capillary extraction of organic vehicle from ceramic bodies.

In the first place eqns (26)–(28) (Part I) were used to calculate the permeabilities of the two powder assemblies at full saturation. For MA2LS and RA6 the ratio  $K_p(\text{liquid})/K_p(\text{gas})=0.25$  was applied to take into account the discrepancy between liquid flow and gas flow permeabilities which was noted for these powders in Part I.<sup>1</sup> The corresponding ratio for LA75 powder was 0.63.

The permeabilities at experimental saturations were then calculated in the same way, and these appear in Table 3 (row 4). These values suggest that, at the start of extraction, the powder beds control the flow, and this is in agreement with the experimental observation that saturation is constant throughout the body during extraction, as shown in Fig. 4. Wax appears to be able to redistribute itself rapidly within the body when loss is from one face. As the saturation of the ceramic body falls, however, its permeability also falls and at the start of the stable stage ( $s=0.9$ ) the permeability of the body is  $2.0 \times 10^{-14} \text{ m}^2$ , which is still higher than that of both powder beds. Again at the end of the stable stage ( $s=0.24$ ) the permeability of the body is  $1.3 \times 10^{-15} \text{ m}^2$ , still above that of both powder beds. However, this involves a long extrapolation. The reduction in permeability of the body at low saturations is another factor bringing about the end of the stable parabolic stage.

The experimental sorption constants in Table 2 were substituted, along with the calculated permeabilities, the porosity and saturation values for the powder beds, into eqn (9), which is the expression for the sorption constant in eqn (8) when the powder bed controls the rate of flow. Wax viscosity at 80°C was 3.78 mPa s,<sup>1</sup> and surface tension was taken as 29 mJ m<sup>-2</sup>.<sup>9</sup> Table 3 (row 5) gives the values of  $\Delta P_c$  calculated therefrom. These seem to suggest that

Table 3. Calculated permeabilities and capillary pressures

Properties	Ceramic body MA2LS	Powder beds	
		RA6	LA75
(1) Porosity	0.46	0.70	0.71
(2) Saturation	1.0 <sup>a</sup>	0.54	0.41
(3) Permeability at $s=1$ (from Part I) (m <sup>2</sup> )	$2.7 \times 10^{-14}$	$5 \times 10^{-13}$	$2.0 \times 10^{-12}$
(4) Permeability at experimental saturation using eqns (26)–(28) (from Part I) (m <sup>2</sup> )	$2.7 \times 10^{-14a}$	$3 \times 10^{-16}$	$2.3 \times 10^{-17}$
(5) $\Delta P_c$ from experimental sorption constant and permeability in (4) (kPa)	—	27	30
(6) Capillary pressure from the Leverett function at $s=0.9$ (kPa)	4.8	11.7	6.6
(7) $\Delta P_c$ calculated from (6) (kPa)	—	6.9	1.8
(8) Permeability calculated from experimental sorption constant and $\Delta P_c$ in (7) (m <sup>2</sup> )	—	$1.2 \times 10^{-15}$	$3.8 \times 10^{-16}$

<sup>a</sup>At the start of extraction.



substantial pressures can be developed, although it will be suggested that these values are overestimated, dependent as they are on values of permeability at  $s < 1$ .

An interesting feature of the experimental results is that the coarse powder LA75 is able to extract molten wax from a body consisting of a finer powder. This is at first surprising because it implies that a continuous fine pore network is available in the powder bed. Figure 1(a) in Part I<sup>1</sup> suggests that the particles may contain porosity. The high capillary pressure is developed in a small fraction of the available pore space, which has an associated low permeability. It is not therefore an ideal powder, as the low sorption constant shows.

The calculation of capillary pressure at saturations less than unity requires the use of the Leverett equation. Table 3 (row 6) gives values of  $P_c$  at the experimental saturations for the powder beds, and for the intermediate saturation at the start of the stable stage for the ceramic body ( $s = 0.9$ ). From these values  $\Delta P_c$  can be calculated (row 7) and turns out to be much lower than the value calculated from the sorption constants. The Leverett function uses permeability at full saturation, which has been determined experimentally in Part I. The extrapolation from  $E_a = 0.58$  to  $0.46$  for the MA2LS powder is not excessive and anyway the porosity dependence of permeability for this powder is low. On the other hand, the calculation of  $\Delta P_c$  from the experimental sorption constant requires a value of permeability at reduced saturation. If the values of  $\Delta P_c$  obtained from the Leverett function are substituted into the expression for sorption constant, higher permeability estimates for the powder beds are obtained (row 8). These are probably better estimates but the absence of permeability–saturation curves impedes further quantitative assessment.

The sorption constants can be estimated using (a)

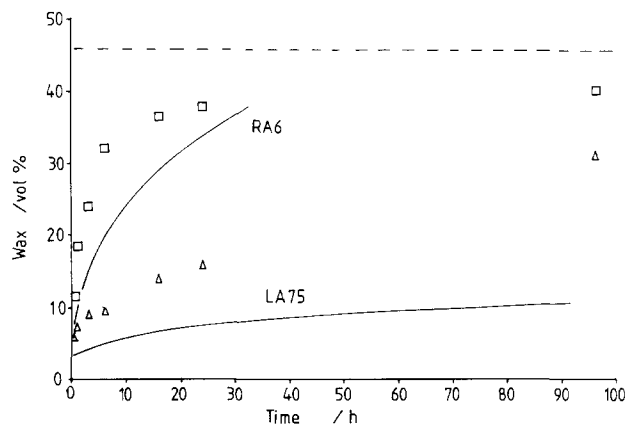


Fig. 5. Calculated flow curves for RA6 and LA75 powder beds and experimental points ( $\square$ , RA6;  $\triangle$ , LA75).

the Leverett function for  $\Delta P_c$  and (b) the permeability—porosity relationships for  $K_p$ , and this gives values of  $K = 1.7 \times 10^{-5} \text{ m s}^{-1/2}$  for RA6 and  $K = 2.1 \times 10^{-6} \text{ m s}^{-1/2}$  for LA75 in conjunction with the MA2LS ceramic body. The flow curve using values of  $V_0$  from data in Fig. 2 and the calculated sorption constants is shown in Fig. 5 and compared with the experimental curve from Fig. 1. The estimate for RA6 is acceptable for the duration of the stable stage, but for LA75 the predicted values are much lower than those observed.

Since the stable stage lasts until about 60% of the available wax has been removed from the ceramic body, the debinding time is best characterized by  $t_{50}$ , the time required for the exodus of 50% of the available wax. Thus

$$t_{50} = \left( \frac{0.5V_i - V_0}{KA} \right)^2 \quad (12)$$

where  $V_i$  is the initial volume of wax in the body,  $V_0$  is the volume of wax removed in the transient stage and  $A$  is the cross-sectional area of the flow path.

Using the calculated sorption constants and taking  $V_0$  as  $0.1V_i$

$$t_{50} = \left( \frac{0.4V_i}{KA} \right)^2$$

Values of  $t_{50}$  are 11.2 and 735 h for RA6 and LA75, respectively. The values deduced from experimental measurements were 2.1 and 46.6 h for RA6 and LA75 powder beds, respectively, indicating that error in  $t_{50}$  is sensitive to inaccuracy in estimates of  $K$ .

#### 4.5 Influence of properties of the organic vehicle on capillary extraction

From eqn (9) it can be seen that

$$K^2 \propto \gamma/\eta \quad (13)$$

and hence the time  $t$  needed to remove a particular amount of organic vehicle

$$t \propto \eta/\gamma \quad (14)$$

Both viscosity and surface tension decrease with increasing temperature. The temperature dependence of viscosity can be expressed by free volume theories or by an activation energy. Although the latter approach has attracted severe criticism<sup>10</sup> it continues to provide a useful predictive fit to experimental data over narrow temperature regions. Thus

$$\eta = \eta_0 \exp(\Delta H/RT) \quad (15)$$

where  $\eta_0$  is a constant and  $\Delta H$  is the 'activation

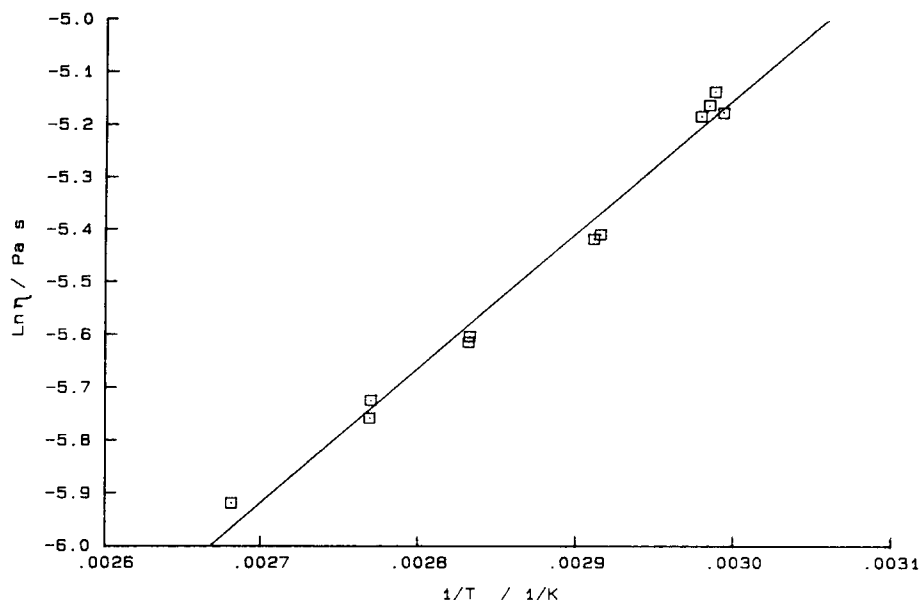


Fig. 6. Logarithm of wax viscosity for  $\square$  RA6 and  $\triangle$  LA75 powder beds plotted as a function of reciprocal temperature.

energy' for viscous flow. Viscosity measurements were carried out in the region 62 to 100°C and the results are plotted in Fig. 6, giving an 'activation energy' of 21.3 kJ mol<sup>-1</sup> and a pre-exponential constant of  $2.66 \times 10^{-6}$  Pa s.

The surface tension of low molecular weight liquids is related to temperature by<sup>11</sup>

$$\gamma = \gamma_0(1 - T/T_c)^{11/9} \quad (16)$$

where  $\gamma_0$  is the surface energy at zero temperature and  $T_c$  is the critical temperature. Thus the temperature coefficient is

$$-\frac{\partial \gamma}{\partial T} = \frac{11}{9} \frac{\gamma_0}{T_c} \left(1 - \frac{T}{T_c}\right)^{2/9} \quad (17)$$

which, for low molecular weight liquids, is about  $0.1 \times 10^{-3} \text{ J m}^{-2} \text{ K}^{-1}$  and for polymers is  $0.05\text{--}0.08 \times 10^{-3} \text{ J m}^{-2} \text{ K}^{-1}$ .<sup>11</sup>

Figure 7 shows how the amount of wax removed in a 6-h period changes with temperature. For the RA6 powder bed there is a 10% increase in the temperature range 70 to 120°C. For the LA75 powder bed there is a 31% increase in the same temperature range. The calculated sorption constant increases by 44% in the same temperature region.

It should be noted that molecular weight has a great effect on the viscosity of thermoplastic organic vehicles. For polymers the melt viscosity can be represented approximately by<sup>12</sup>

$$\log \eta = 3.4 \log Mw + A_v \quad (18)$$

where  $A_v$  is a constant. Since the extraction time increases with the same order as viscosity, it follows that the process of capillary extraction is very sensitive to molecular weight and may be unsuitable for higher waxes, and especially for polymers.

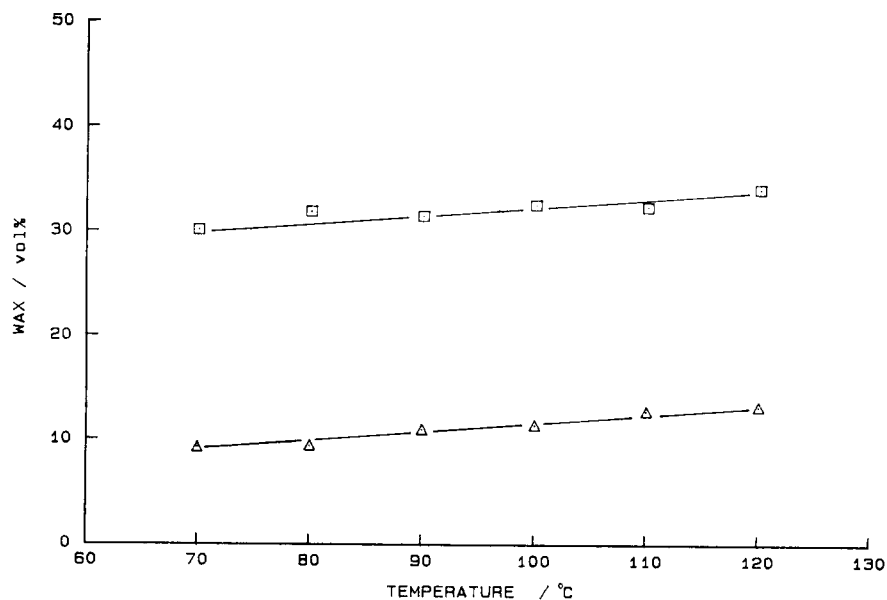


Fig. 7. Amount of wax extracted after 6 h at various temperatures for  $\square$  RA6 and  $\triangle$  LA75 powder beds.

Molecular weight may also influence the obstruction to flow in porous media by adsorption. The hydrodynamic layer thickness is approximately equal to the average chain end-to-end distance<sup>13</sup> in solution studies. A comparable effect is expected in the melt so that the pore architecture may be partially or completely blocked by immobile layers of high molecular weight polymers.

## 5 Conclusions

The rate of extraction of organic vehicle from a moulded ceramic body by a powder bed can be described by three stages: (i) an initial stage of rapid flow, (ii) a stable stage in which the rate is proportional to the square root of time as for extraction from an unlimited supply but with a lower sorption constant, and (iii) a reduced velocity stage in which the flow is impeded by a reduction in the number of transport paths as the liquid columns disintegrate and the wax is present in the body in pendular configuration.

During the stable stage the residual wax is uniformly distributed throughout the body and the loss of wax is accompanied by a decrease in saturation. In contrast, in the powder bed saturation remains constant and a column of liquid advances into the powder. During the stable stage the amount of wax extracted varied with square root of time as for extraction from an unlimited supply but with much lower sorption constants. This occurred because the powder bed controlled the rate of flow and the variation in capillary pressure in the ceramic body is low in the saturation regime associated with the stable stage.

Saturation of the powder beds studied was lower than that observed in absorption from an unlimited supply, and this can be attributed to the wide pore size distribution in loosely packed powders; only the fine pores in the bed can withdraw liquid from the pores of the body. Attempts to calculate the sorption constant from independent experiments are limited

by the absence of permeability–saturation curves for the powders. Thus a general model for the capillary extraction of organic vehicle capable of giving acceptable estimates of the behaviour of diverse powders remains elusive.

## Acknowledgements

The authors are grateful to Brunel University for financial support for Mrs Yuqing Bao as a visiting scholar, and to Mrs K. Armstrong for typing the manuscript.

## References

1. Bao, Y. & Evans, J. R. G., Kinetics of capillary extraction of organic vehicle from ceramic bodies. Part I: Flow in porous media. *J. Eur. Ceram. Soc.*, **8** (1991) 81–93.
2. Wright, J. K. & Evans, J. R. G., Removal of organic vehicle from moulded ceramic bodies by capillary action. *Ceramics International*, **17** (1991) 79–87.
3. ASTM, Standard specifications and operating instructions for glass capillary viscometers. American Society for Testing and Materials, Philadelphia, USA, 1979, pp. 249–55.
4. Edirisinghe, M. J. & Evans, J. R. G., Compounding ceramic powders prior to injection moulding. *Proc. Brit. Ceram. Soc.*, **38** (1986) 67–80.
5. German, R. M., Theory of thermal debinding. *Int. J. Powder Met.*, **23** (1987) 237–45.
6. Shaw, T. M., Liquid redistribution during liquid phase sintering. *J. Amer. Ceram. Soc.*, **69** (1986) 27–34.
7. Leverett, M. C., Capillary behaviour in porous solids. *Trans. AIME*, **142** (1941) 152–69.
8. Carman, P. C., Flow of gases through porous media. Butterworths, London, 1956, p. 56.
9. Kaelble, H. D. & Vy, K. C., A Reinterpretation of organic liquid–polytetrafluoroethylene surface interactions. *J. Adhesion*, **2** (1970) 50–60.
10. Hildebrand, J. S., Operations on swollen theories with Occam's razor. In *Structure–Solubility Relationships in Polymers*, ed. F. W. Harris & R. B. Seymour. Academic Press, New York, 1977, pp. 1–10.
11. Wu, S., Interfacial and surface tension of polymers. *J. Macromol. Sci. Macromol. Chem.*, **C10** (1974) 1–73.
12. Van Krevelen, D. W., *Properties of Polymers*. Elsevier, Amsterdam, 1972, p. 258.
13. Priel, Z. & Silberberg, J., The thickness of adsorbed polymer layers at a liquid–solid interface as a function of bulk concentration. *J. Polym. Sci., Polym. Phys.*, **16** (1978) 1917–25.